SCOUR BEHIND CIRCULAR CYLINDERS IN DEEP WATER

by

JORG IMBERGER
Centre for Environmental Fluid Dynamics
Department of Civil Engineering
University of Western Australia
Nedlands, Perth, WA 6009

DES ALACH
Kinhill Stearns
Engineers
111 St George's Terrace, Perth, WA 6000

JOHN SCHEPIS
Department of Civil Engineering
University of Western Australia
Nedlands, Perth, WA 6009

Abstract

Flume test data is presented for the depth of scour in deep water near a vertical cylinder placed in a uniform sand and a fine calcareous ocean sediment. The ratio of the depth of scour to the cylinder diameter at equilibrium is shown to depend only on the ratio of the shear velocity to the critical shear velocity at which bed motion is initiated.

Protection against scour by placing collars around the cylinder is shown to be of marginal value.

1 INTRODUCTION

Scour around cylindrical piles has long been of importance in the design of bridge piers and ocean jetties (Durant Claye 1873). In most cases investigators have emphasised the influence of the water surface effects and further, most tests have been carried out with sand as the foundation material. With the growth of the off-shore industry there is an increasing need to estimate scour around piles in water which is many pile diameters deep and where the foundation material is made of calcareous particles of a fine sandy consistency by the ocean. Further, scour tolerances on off-shore structures are such that attention must be focused on the range of shear velocities from the inception of scour to values at which bed load motion commences.

Such data do not appear to exist and this need has led to the above general investigation of scour around plain vertical circular cylinders and cylinders with protective collars. The sediment used is typical of that found along the whole of the Western Australian continental shelf in water between 50m and 200m (see H.A. Jones 1973). The photograph in Figure 1a shows that the particles are an approximate size of 0.1mm, are angular in nature and possess irregular shapes. A typical size fraction of these sediments is shown in Figure 1b and Figure 1c shows the size fraction of the fine river sand used in the control experiments.

Recent measurements of velocities very close to the ocean bottom (Caldwell and Chris 1979) have revealed that the bottom boundary layer possesses a "law of the wall" region above the viscous sublayer in which the familiar velocity scaling,

$$u = 2.5u_* \ln \frac{z}{z_o}$$

is applicable, where u is the velocity, u_* is the shear velocity, z is the vertical distance from the bed and z_o is the bottom roughness parameter. These measurements imply that a useful experiment of the scour depth may be carried out in a laboratory flume, provided the depth of water is kept large compared to the cylinder diameter.

The dominant feature responsible for scour around a pile is the large scale eddy system created by the pile itself. It is generally accepted that this eddy system causes the scour around the pile to commence at about half the critical threshold velocity. Shen, Schneider & Karaki (1966) reported that depending on the pile type and free stream

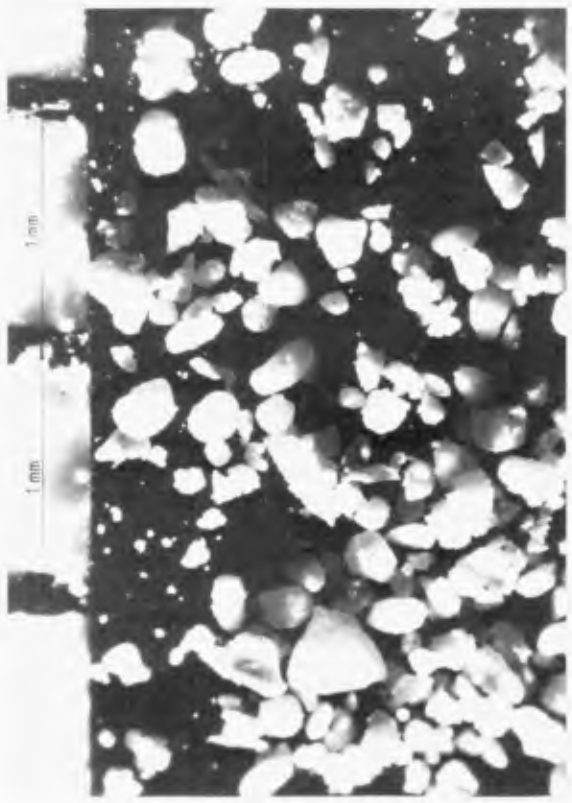

FIGURE 1a

Photograph of ocean sediment.

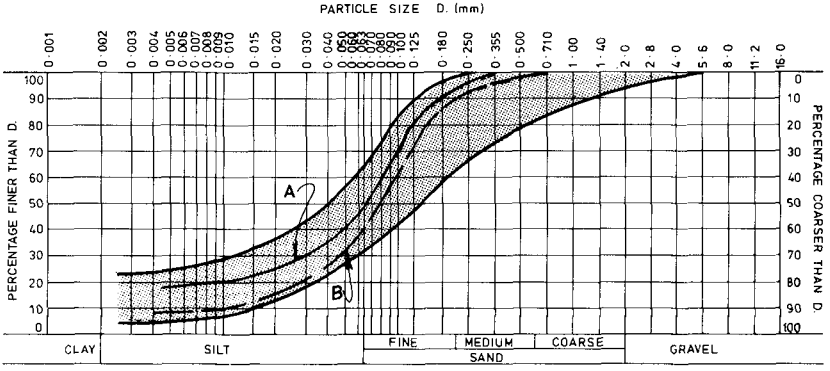

CALCAREOUS SEDIMENT FIGURE 1b

Dry sieve analysis of typical ocean sediment after separating coarse material used in experiments (A: +0.6mm; B: +1.2mm)
From Fugro Report K-1052/XVIII).

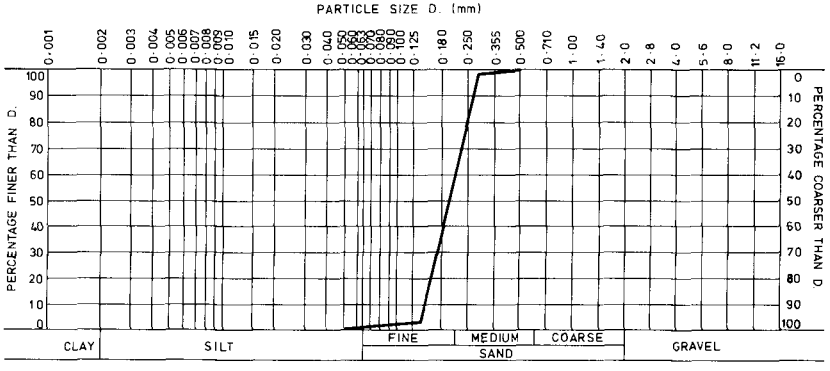

SAND FIGURE 1c

Sand sample particle distribution used as a control soil sample.

conditions, the eddy structure may be broken down into regions of a forward horseshoe vortex, a wake vortex amalgamation and a trailing vortex system.

The horseshoe vortex filament is the major influence on scour around a cylindrical pile. The variations in the intensity of the horseshoe vortex and in the strength of the downflow, and the interaction between them were examined qualitatively by Melville (1975) and reinterpreted by Jain & Fischer (1979).

The horseshoe vortex was reported to be initially small and comparatively weak. When the scour hole forms, however, the vortex rapidly grows in size and strength as additional fluid attains a downward component and the strength of the downflow increases. The expanding cross sectional area increases but, at a decreasing rate as the scour hole enlarges. The rate of increase in the cross sectional area is controlled by the quantity of fluid supplied to the vortex from the downflow ahead of the cylinder. This downflow is determined by the free stream velocity.

The scour resulting from this flow pattern leads to an increasing depth of scour with increasing flow velocity. However, as shown by Shen et al (1969), there is some doubt whether scour continues once the critical shear velocity is exceeded. Their results are at variance to those of Jain and Fischer (1980), but there is some evidence that once an active bed load has been established the rate of filling equals the rate of scouring and a type of scour equilibrium is reached. The reader is returned to the article by Breusers, Nicollet and Shen (1977) for a good comprehensive summary.

Thomas Zdenek (1967) examined the influence of protective collars and presented data for two collar sizes. The results showed that scour still occurred around the pile under the collar but of a lesser depth. With the collar directly on the bed at $u_* = u_{*_c}$ and $D_c/b = 3$, where u_{*_c} is the critical shear velocity, D_c is the diameter of the collar and b is the diameter of the cylindrical pile, the scour depth was reduced to 24.6% of the scour which was recorded when no collar was present.

A similar reduction was observed by Tanaka and Yano (1967).

Scour around deep ocean structures can thus not be determined from previous work. Little data exists for small surface Froude numbers, although an introductory discussion may be found in Carstens and Sharma (1975). Experiments on interlocking-type soils in flows with a small surface Froude number are thus required. Such an investigation was carried out and is described in this paper.

2 EXPERIMENTAL DESIGN

Scour behind a vertical cylinder depends on the sediment structure and composition, the mean velocity field, the turbulent velocity field in the water column and the shape of the structure. Defining the depth of scour as d_s and the diameter of the cylinder as b it is possible to write,

$$d_s/b = f(u_*, u_{*c}, u, g', d_{50}, h, \nu) \tag{1}$$

where u_* is the shear velocity, u_{*c} is the shear velocity at which bed motion is initiated over an unobstructed bed, u is the free stream velocity, g' (= $(\frac{\Delta\rho}{\rho})g$) is the effective acceleration due to gravity of the sediment particles, $\Delta\rho$ is the density difference between the sediment and the water, ρ is the density of the water, d_{50} is the median particle size, h is the depth of flow and ν is the kinematic viscosity.

In writing equation (1) it is assumed that the sediment structure and particle size distribution are characterised by the parameters u_{*c} and d_{50}. Cohesive soils are not considered in the present discussion. Further, the mean flow profile and the turbulent kinetic energy field are assumed to be that described by the "law of the wall" and so are completely characterised by the shear velocity u_*.

Invariance to a transformation of the dimensions requires that equation (1) may be written in the form:

$$d_s/b = f(u_*/u_{*c}, u_*^2/g'd_{50}, h/b, ub/\nu, d_{50}/h), \tag{2}$$

where the dimensional groups have been chosen to reflect the most likely force balances. In the order in which the groups appear in equation (2) the following interpretations are noteworthy:

a) u_*/u_{*c} is the ratio of the applied shear velocity to the value at which motion is initiated on a flat bed. This ratio captures the influence of the drag force exerted by the flow on the sediment bed as a fraction of the stress required to move the sediment without flow disturbances due to the structure. Scour usually commences at shear velocities well below the critical value because the cylinder induces a locally higher value immediately adjacent to the perimeter. The value of u_{*c} captures the erosion resistance characteristics of the sediment and so will not only depend on the sediment type and size, but also on its gradation and the final packing.

b) $u_*^2/g'd_{50}$ is the ratio of the inertia force on a sediment particle associated with the turbulent fluctuations of the flow to the effective weight of a sediment particle. The turbulent fluctation possesses velocities of the order of u_* and so the inertia term is merely a reflection of the form drag (pressure $0(\rho u_*^2)$ multiplied by the area presented by the particle) on the sediment particle.

c) h/b is the depth to cylinder diameter ratio. The importance of this parameter lies in the fact that as this boundary layer flow is intercepted by a vertical structure, the stagnation pressure at the leading edge of the structure will vary from ρu^2 in the core flow to 0 at the sediment base. This pressure difference is experienced by the flow over the velocity transition layers leading to a vertical pressure gradient at the leading edge of the structure of $0(\rho u^2)$. This pressure gradient induces a vortex motion of radius r_o which is swept around the pile forming a trailing vortex pair in the wake of the structure. The velocities associated with this trailing vortex pair combine with the mean flow causing a local increase of u_* in the immediate lee of the structure.

d) ub/ν is the cylinder Reynolds number. For Reynolds number larger than about 10^3 little effect may be expected until a value of 10^5 is reached. For values greater than 10^5, the separation is retarded by the turbulent boundary layer and the rear wake is somewhat narrower than that which would be expected from a laminar boundary layer. The pressure field in the wake arising from this separated flow combines with that from the trailing vortex pair to produce the observed total flow.

e) d_{50}/h is the relative roughness of the bed material. In coarse materials this parameter determines the turbulent structure in the bottom boundary layer. For the calcareous sediment and the sand under study the median diameter d_{50} ranges from 0.04 - 0.125mm and 0.25mm respectively implying that for smooth flat beds the flow is hydrodynamically smooth and the parameter d_{50}/h is of minor importance. For strongly roughened or pitted surfaces, however, a new parameter e/h must be added. The variable e is used to designate the roughness height of the undulations.

In the strictest sense the depth of scour will depend on all of the above parameters as well as possibly the sediment structure. However, interest here is centered around deep water structures for which h/b is large. Assuming experiments are not carried out at the critical Reynolds number, it may thus be expected that equation (2) reduces to the form:

$$d_s/b = f(u_*/u_{*c}, u_*^2/g'd_{50}) \tag{3}$$

and all other variables would be small scale effects. The experiments were designed to investigate the form of the function in equation (3).

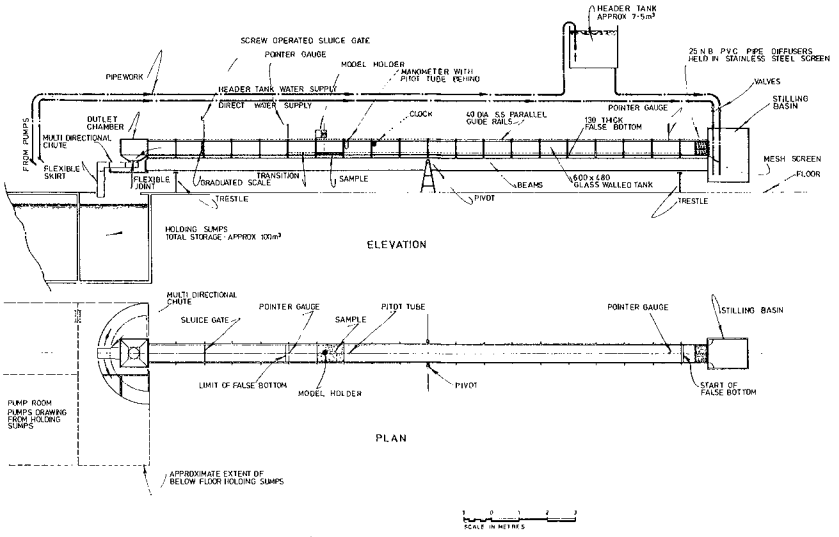

FIGURE 2 General arrangement of test flume.

3 EXPERIMENTAL PROCEDURE

The model tests were carried out in the Hydraulic Laboratory of the Department of Civil Engineering at The University of Western Australia. The experiments necessitated the construction of a 20m tiltable glass walled flume, the installation of a pitot-static tube and the design of sediment sample preparation techniques.

Experimental Flume and Apparatus

The general layout of the experimental test flume is shown in Figure 2. The flume consisted of a 20m long test section with a cross-section 600mm wide and 480mm deep. All tests were carried out with the flume in a horizontal position. The supply of water for the flume came from the laboratory storage tanks beneath the laboratory floor and was routed to the header tank of the flume via two pumps. Under normal operating conditions the system allowed the level in the flume to be kept constant to approximately $\pm$2mm. From the header tank the water moved through a converging entrance into the flume section through a multiple pipe diffuser installed in the first bay of the test section. The purpose of the pipe diffuser was to dissipate any wave action and uneven flow that may have arisen from the introduction of the water into the header tank.

The normal way of operating the flume was to set the downstream sluice gate at predetermined openings (15mm, 30mm, 50mm, 85mm, 100mm and 115mm) and then to adjust the two valves at the inflow to yield a full depth test. In this way it was possible to repeat experiments with almost identical flow conditions.

The flume was fitted with two surface rails accurately aligned allowing equipment to be positioned accurately within the flume. The pointer gauge, the pitot tube and the test section were all fitted in the flume from specially constructed trolleys running on the rails.

In order to be able to fit a 100mm deep sediment tray into the flume bed for the tests, it was necessary to construct a false bottom for most of the upstream part of the flume. This false bottom was constructed for 3m upstream and 1m downstream of reinforced P.V.C. sheeting. Upstream of this the flume bed was lined with bricks which were covered with a thin grout to yield constant depth of flow. The false bottom was painted and then while the paint was still wet, sprinkled with dry sediment. After drying, the surface remaining on the paint very closely resembled a smooth sediment surface with the same roughness properties as the sediment itself. Great care was taken to ensure that all the joints were smoothly aligned and that the sediment test section which fitted into the

false bottom through a cavity was accurately placed. The small gaps left were filled with plasticine to ensure a smooth, flat bed.

Sediment Tray

It was realised at the outset of the experiments that it would not be possihle to deposit sediment in the total length of the flume. Although this would have been advantageous in that it would have allowed tests to be carried out above the critical shear velocity, the logistics for obtaining such large quantities of deep ocean sediment and further of depositing the sediment in the flume made this impracticable. It was therefore decided to construct a test pan 100mm deep and 1m long which fitted across the flume. The material was sieved and redeposited into this test tray as described below after which time the tray was lifted with a small crane and positioned into the cavity of the false floor. The tray was constructed of reinforced fibreglass with a strong structural base to ensure no movement of the tray base occured during installation of the tray.

The Pitot Tube

The velocity in the flume was measured with a standard pitot-static tube with an outside diameter of 4mm. The pressure difference in the pitot tube was measured with a differential manometer. This manometer was filled with turpentine which had a specific gravity at room temperature of 0.808. The use of turpentine and water allowed accurate measurement of velocities even down close to the viscous sub-layer. The surface tension effect was minimised by choosing 10mm diameter tubes for the manometer. This meant that the instrument also had a large damping time allowing easy determination of the mean velocity profile.

Test Cylinders

The test cylinders were straight circular cylinders with diameters of 25mm, 50mm and 100mm with and without circular metal collar discs 3mm thick. The discs had diameters twice, three and four times the diameter of the cylinders and were made to allow for positioning at various heights above the upper surface of the sediment when the model structure was in position.

The leading edge of each of the model cylinders was fitted with a sharp V lip which was ground to a very fine edge in order that the whole circumference of the model would cut through the sediment with minimum disturbance during installation. A small hole was drilled through the upper flange of the model to allow the air to escape as the cylinder

was inserted into the sediment. This avoided possible compaction of the soil within the centre of the cylinder and the consequent disturbance of the soil adjacent to the cylinder wall by bearing capacity failure.

Sample Preparation

The 100mm thick calcareous sediment samples were prepared by a wet "sand rain" technique in an attempt to reproduce the natural method of in-situ deposition of the coastal sediments. This method is similar to the conventional dry "sand rain" technique used for uniform granular samples (Jewell et al (1980)).

A mass of 1.00kg of the sediment which had been packed wet and sealed after collection at sea was wet further to a moisture content of approximately 60% and moulded into a slurry. This slurry was spread uniformly onto a No. 14 mesh screen of exactly the same dimensions as the sample tray and then washed through the sieve with fine water jets into the tray below. After allowing at least 45 minutes for the finest particles to settle, all water more than approximately 5mm deep over the sample was siphoned off and the next layer was rained in until the prepared sample was at least 5mm above the top of the tray top lip. When the sample was required in the flume for testing, the excess water was siphoned off, the skirt removed from the tray and the soil above the top lip of the tray cut off. This was achieved by moving a vibrating cutter fitted with a vacuum system across the top of the tray producing a smooth surface without evidence of tearing or drag marks on the sample surface. The prepared sample tray was then weighed and lifted into the flume for testing. The average void ratio achieved by this method in the large sample trays was 1.73 which was somewhat higher than the understood typical field value of 1.35, with the layering and structure being reproduced rather well.

The control tests were carried out with clean, dry, uniform sand sieved to provide a d_{50} of 0.2mm. This was poured slowly into the sample tray which had previously been filled with water, vibrated vigorously on a vibrating platform normally used for preparing concrete test cubes, trimmed to height with a straight edge and then lifted into the flume for testing. The particle size distribution for this sand was almost linear between 0.125mm and 0.3mm.

Flume Performance

In order to verify the performance of the flume a number of tests were carried out to check the logarithmic profile above the smooth plastic false bed, the fixed sand sediment bed and the actual sediment tray. Table 1 summarises the results from this test and gives

TABLE 1 Flume performance data.

Code	Bottom			Flow Depth	Water Temp.	Flow Vel.	Shear Vel.	Measured roughness	$\frac{9z_o u_*}{\nu}$	Date of Test
	Material	d	d_{50}	H	T	$u_{0.1}$	u_*	z_o		
		m	m	m	^oC	$msec^{-1}$	$msec^{-1}$	m		
		10^{-3}	10^{-3}	10^{-3}		10^{-3}	10^{-3}	10^{-6}		
S3-a	P.V.C.			300	15.5	129	6.3	28.0	1.30	23.8.81
S3-b	P.V.C.			275	15.5	278	12.0	9.4	0.99	23.8.81
S3-c	P.V.C.			190	15.5	535	22.0	6.1	1.15	23.8.81
S7	Fixed Sed.			307	15.5	555	22.6	4.9	0.71	8.9.81
S17	Fixed Sed.			307	16.0	526	21.6	5.8	1.06	29.9.81
S5	Sed.	15	0.06	207	16.0	560	23.9	8.6	1.56	27.8.81
S6	Sed.	50	0.06	225	16.0	549	21.9	4.3	0.98	28.8.81

Test Result Summary: Flume Performance

the flow depth, the water temperature, the flow velocity at 100mm, the shear velocity as calculated from the slope of the velocity profile, the measured roughness as calculated from the intercept of the velocity profile with the velocity axis and the last column gives the ratio of the measured roughness length, z_o to that predicted for a smooth bed. The velocity profiles were logarithmic as shown in Figure 3, and in general the effective roughness was in good agreement with the theory (see Table 1).

Test Results

All together 22 scour tests were carried out with the following configurations:

a) Circular cylinders in uniform sand.
b) Circular cylinders in ocean sediment.
c) Circular cylinders with a circular collar disc at the level of the ocean sediment surface.
d) Circular cylinders with a circular collar disc at a given distance off the ocean sediment surface.

In each case the soil tray was placed into position and the flume carefully filled with water with the sluice gate closed. The model cylinder was then inserted into the sediment, care being taken not to unnecessarily disturb the sediment. The tests were started by setting the sluice gate to a 15mm opening and adjusting the depth of flow with the upstream valves. Normally, tests were carried out with sluice gate openings at 15, 30, 50, 85, 100 and 115mm. Each test was recorded on video tape for later reference. The velocity corresponding to each sluice gate setting was measured at a height of 100mm from the channel floor with the pitot tube attached to the manometer and the shear velocity was determined by assuming a logarithmic velocity profile. The scour contours were sketched as the experiment proceeded and the depth of the deepest scour hole was recorded for each equilibrium situation. The velocity was raised in the channel until either scour had reached the sediment tray bottom (100mm) or until the shear velocity was equal to or a little greater than the critical shear velocity. Tests for shear velocities above the critical value could not be carried out as the experimental apparatus had no provision for upstream sediment replenishment.

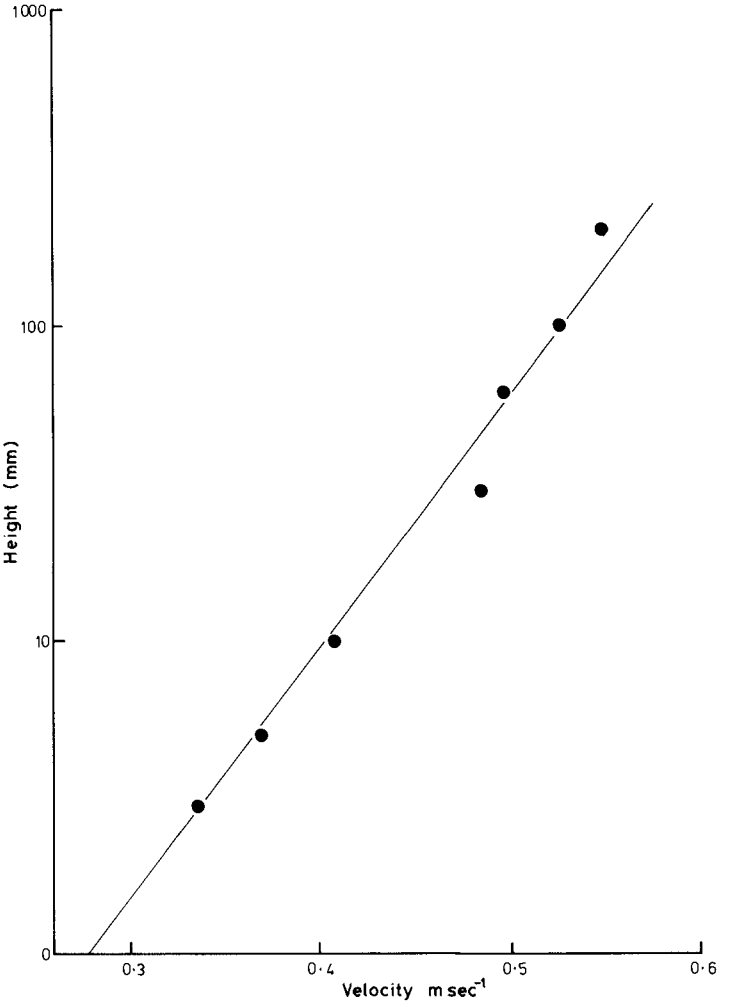

Velocity distribution over a fixed sediment bed.

4 RESULTS

The Critical Shear Velocity

The critical shear velocity is defined as that shear velocity at which the particles on the bed begin to consistently move. In the case of the sand bed the initiation of motion was well defined and little ambiguity existed regarding the determination of the critical value of the velocity. Two separate tests, specifically conducted to determine the critical shear velocity, yielded values of 13mmsec^{-1} and 15mmsec^{-1} respectively. These values may be compared with the prediction from the Shield's diagram (Vanoni, 1975) of 13mmsec^{-1} for a uniform sand of 0.2mm median diameter. A value of 13mmsec^{-1} was chosen for the data reduction of the sand scour tests.

The determination of the critical shear velocity for the calcareous sediment was made difficult by the very patchy nature of the initiation of the bed particle motion. Distinct from sand this material formed small scour depressions when close to the critical shear velocity. These depressions deepened to about 1mm and widened to an elongated ellipse with a size of about 300mm in length and 10mm wide. At this stage further movement stopped and the activity shifted to other parts of the bed. It was therefore difficult to judge the exact value of the critical shear velocity, but two test trays yielded critical shear velocities of 24mmsec^{-1} and 23mmsec^{-1} respectively. During the whole range of the other scour tests conducted these values were repeatedly confirmed and so a critical velocity of 23mmsec^{-1} was chosen for all the data reduction.

This value of the critical shear velocity for the calcareous sediment may be compared to the prediction of 12mmsec^{-1} from the Shield's diagram for a uniform sand with an equivalent diameter of 0.06mm. The calcareous sediment therefore derived from the interlocking of the particles an appreciably higher resistance to erosion than sand of equivalent size.

Scour Near A Circular Cylinder: Sand

Three sand scour tests were conducted mainly as control to enable comparisons with published data.

The scour patterns from all the tests were geometrically similar. The final depression for a test with the 50mm diameter cylinder is shown in Figures 4a and 4b where it is seen that the majority of the material which scoured out from near the cylinder was redeposited immediately to the rear of the scour depression.

FIGURE 4a Photograph of sand scour depression around 50mm cylinder at maximum u_*.

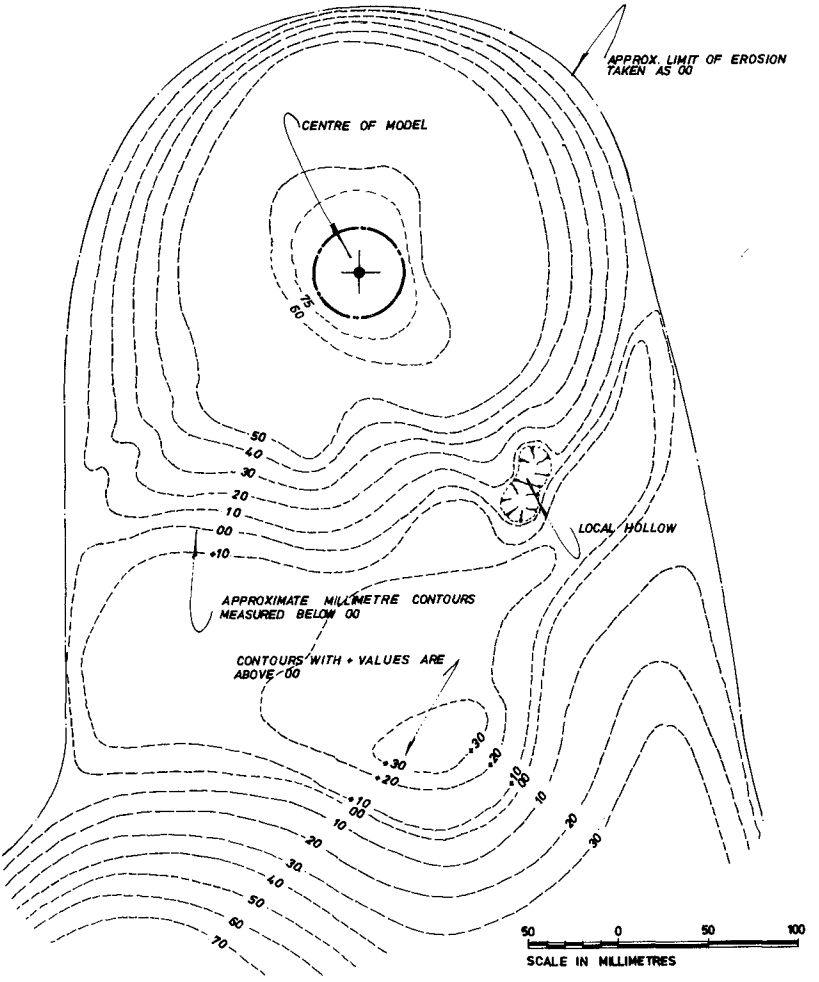

Sketch of sand scour depression contours around 50mm cylinder at maximum u_*.

The vortex motion and turbulence was seen to lift the sediment into suspension near the cylinder wall and the mean current carried the material out of the depression. This removal of material from the base of the depression always resulted in a slope adjustment further up the depression which replenished the areas where scour had taken material away. This process, as shown in Figure 4a, was symmetric and the scour depression was cone-shaped. Interesting radial depressions formed around the perimeter of the cone due to the presence of radial vorticity, but no detailed investigation of this mechanism was undertaken (see Figure 4b).

The equilibrium maximum scour depths are shown in Figure 5 for the tests with 25mm, 50mm and 100mm diameter cylinders. The data was plotted according to equation (3) and it is seen to display a linear trend with scour commencing at a value of $u_*/u_{*_c} = 0.5$.

Scour Near A Circular Cylinder: Sediment

The evolution of scour was characterised by a beginning of scour at the rear and either side of the cylinder. This happened at a u_*/u_{*_c} of approximately 0.3 to 0.4. As the velocity in the channel was raised the scour depression deepened at the rear and moved forward around the perimeter of the cylinder. The mode of deepening was similar in all cases. Small depressions would form locally, deepen up to 5mm and then broaden to the outer boundary of the depression. This led to sheet like striations at the edge of the scour depression as is seen in Figure 6a. This photograph also clearly shows a local depression next to the cylinder in the deepest part. The forward bank tended to be very steep and the spoils from this scour did not resettle in any of the experiments, but were swept downstream into the sump (see Figure 6b). This is further evidence that the particles interlock, giving the bed an erosion resistance far greater than the equivalent sand. The shear stress required to break this interlocking is considerably higher than that required to transport the particles once loose. This is in contrast to the sand case, in which the scoured sand was mostly deposited immediately in the lee of the scour depression indicating that the scour stress was only marginally higher than the transport stress.

The thickness of each scour layer evident in Figure 6a is many times greater than the individual layering introduced during sample preparation and it is not likely that the sample preparation formed the layers.

It is seen from Figure 7 that the data from the different tests form a linear correlation between d_s/b and u_*/u_{*_c} independent of the internal particle Froude number. The line of best fit is given by the equation:

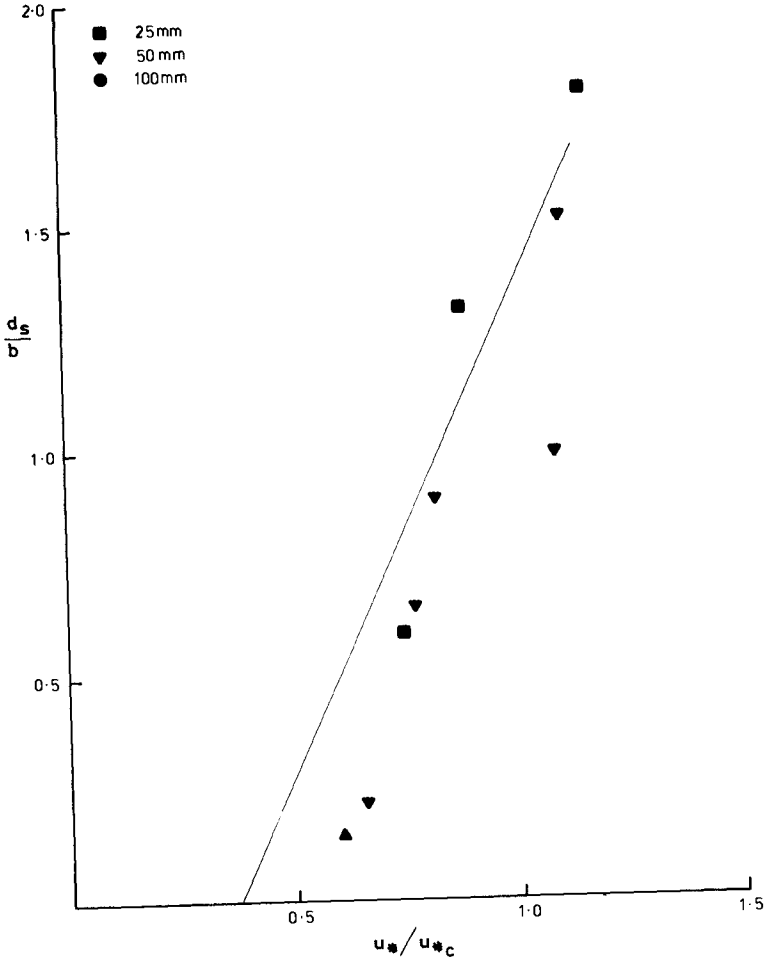

Dimensionless plot of scour depth against the shear velocity for a circular cylinder in 100mm deep sand.

FIGURE 5.

FIGURE 6a Photograph of ocean sediment scour depression around 50mm cylinder at maximum u_*.

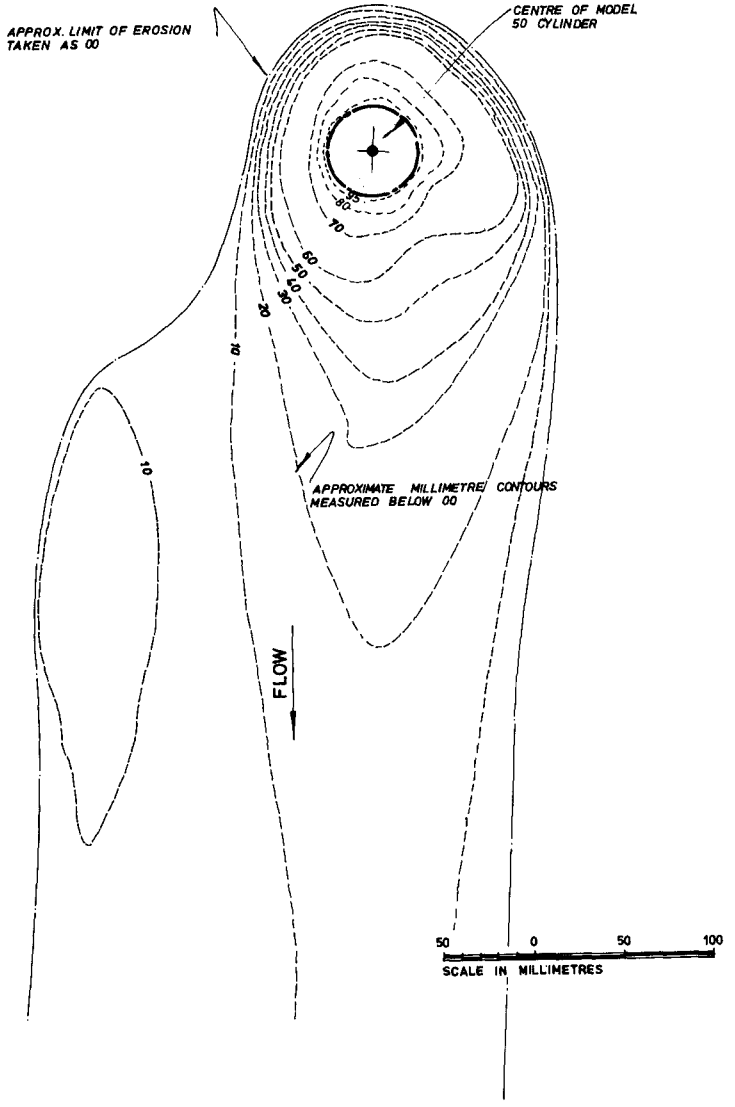

Sketch of ocean sediment depression contours around 50mm cylinder at maximum u_*.

FIGURE 6b

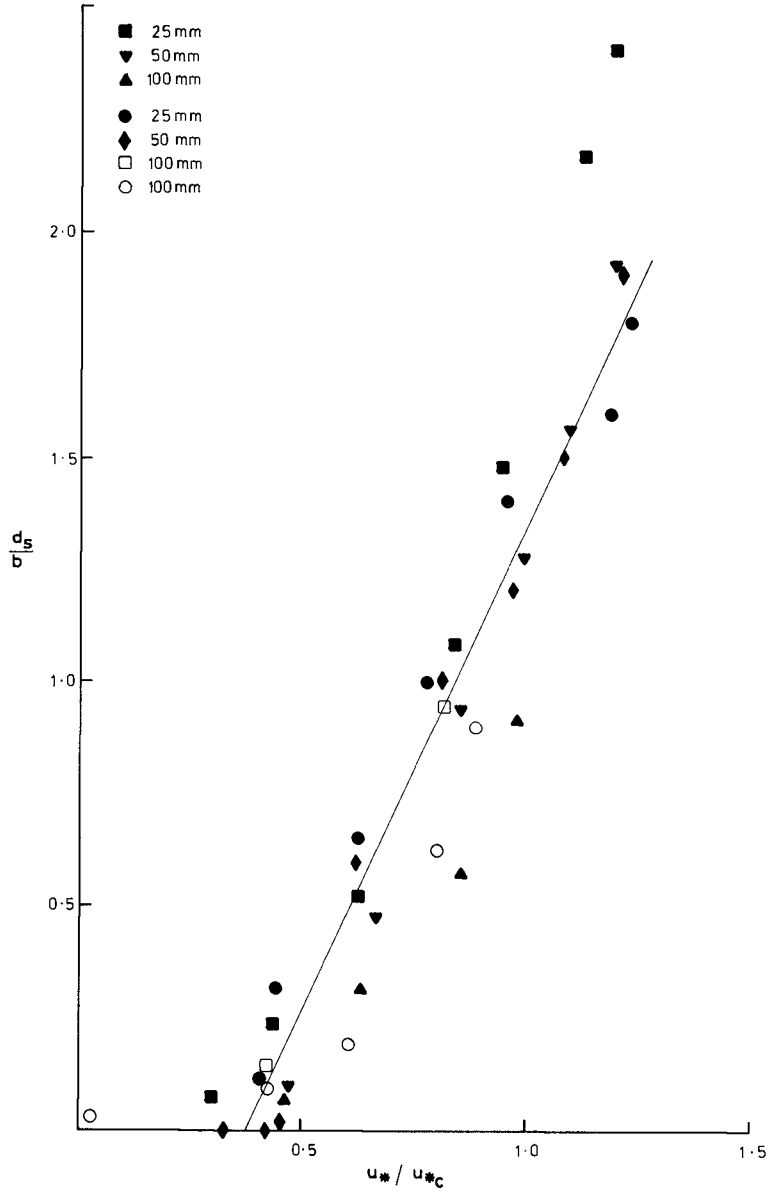

Dimensionless plot of scour depth against the shear velocity for a cylinder in 100mm deep ocean sediment.

FIGURE 7.

$$d_s/b = B(u_*/u_{*c} - 0.374) \quad (4)$$

where the constant B = 2.18.

Effects of Collars on Scour Depth

Visualisation of the flow with dye streaks clearly showed the formation of a horseshoe vortex around the front of the cylinders which was then swept around the perimeter of the cylinder. In the wake the vortex filaments combined to give a fairly confused wake with a peak outward flow at the bed of about half diameter in the lee of the cylinder and spaced approximately one third cylinder apart.

It was postulated that placing a metal collar around the cylinder should protect the bed from this increased flow intensity and so a series of experiments were conducted with differing collar to cylinder diameter ratios and at three levels; tests were carried out with the collar level with the bed, 20mm from the bed and one with the collar at 60mm from the bed.

Scouring for all collar ratios, with the collars at bed level, started at a u_*/u_{*c} of about 0.4 with this initial scour occuring downstream of the collar within the wake region. Initial scour did not occur as for the plain cylinder but rather resembled a surface scraping process in the wake region well away from the collar perimeter. As the flow was increased, the scour area widened and moved upstream up to the collar eventually undermining the downstream half of the collar area. For collar to cylinder diameter ratios of 3 and 4 the scour depression widened very considerably as seen in Figure 8, leading to a depression width of 2-3 times the diameter of the collar. Reduction of the diameter ratio led to progressive movement of the scour depression upstream under the collar into the cylinder. For the case of a ratio of 2 scour occured around nearly three quarters of the cylinder immediately below the collar.

The equilibrium depth for a particular shear velocity was always achieved by a central deepening and then a progressive widening. The final scour depths are shown in Figures 9a, b and c for the different collar to cylinder diameter ratios.

From these diagrams it is seen that scour commenced at much the same value of u_*/u_{*c} as with no collar, but the rate of scour was slower until d_s/b of about 1 where upon scour seemed to increase. Although it was not possible to attain in the present facility, the data indicate a trend back towards the cylinder without collar curve for ratios of d_s/b

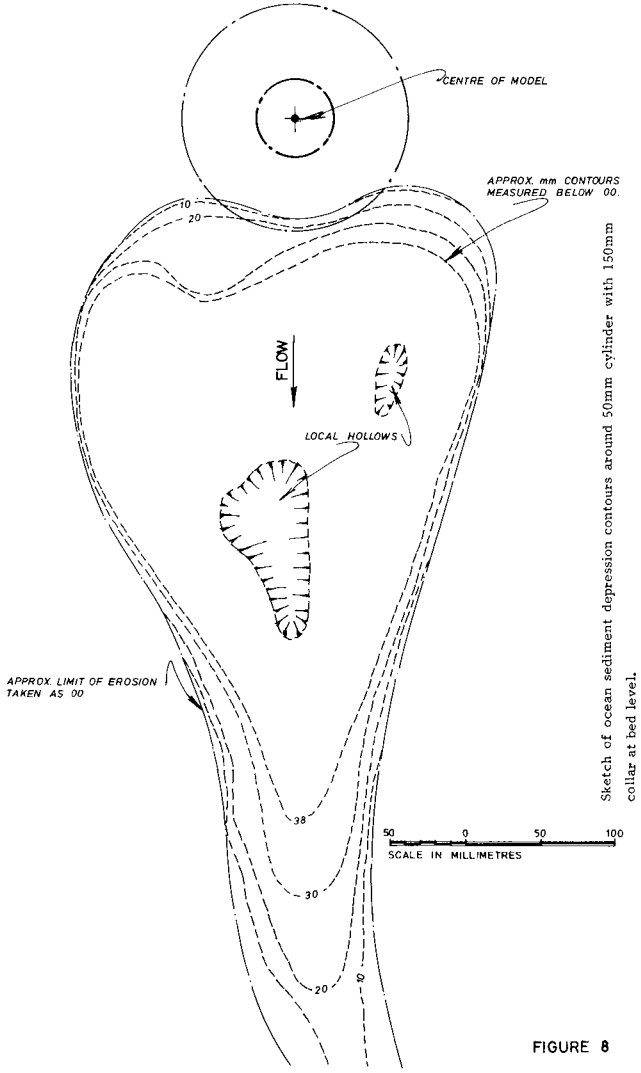

Sketch of ocean sediment depression contours around 50mm cylinder with 150mm collar at bed level.

FIGURE 8

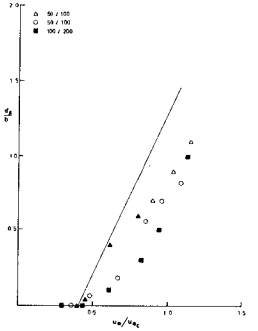

Dimensionless plot of wave depth to ocean sediment against the shear velocity for cylinders with rafting at bed level.
(a) $D_c/D = 2.0$ (b) $D_c/D = 3.00$ (c) $D_c/D = 4.0$

FIGURE 9a

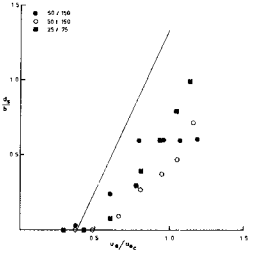

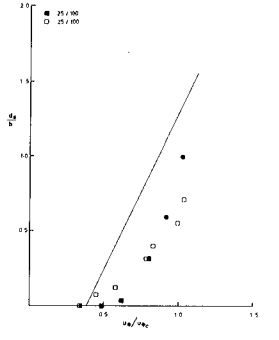

FIGURE 9c

larger than about 1. The scour retardation seemed to be more marked the larger the value of d_s/b.

To investigate the transition back to the plain cylinder case, the effective d_s was increased by raising the collar 20mm above the sediment bed. The results from these tests are shown in Figure 10. All ratios of d_s/b are included and it is seen that there is a general trend back to the plain cylinder line until at d_s/b of about 1.5 the scour depth is back to that found in the plain cylinder case. The scour process in the raised collar tests differed very little to that described above for the level collar tests. For the ratio d_s/b = 3 and 4 the scour developed at the perimeter of the cylinder after which it became localised in the region directly under the collar. For the ratio d_s/b = 2 the scour was very erratic, most probably due to the added turbulence caused by the edges of the collar.

The tests with the 50mm diameter cylinder indicated a disappearance of the effect of the collar at d_s = 75mm to 80mm. Subtracting the 20mm, would imply that a 50mm diameter cylinder with a collar at 60mm height would show no effect of the collar. The results shown in Figure 10 substantiate this conclusion, indicating that the horseshoe vortex is affected by plates or collars for a distance above the bed of about 1.5 times the cylinder diameter. This is considerably larger than the horseshoe vortex diameter ratio of 0.25 predicted by Qadar (1981).

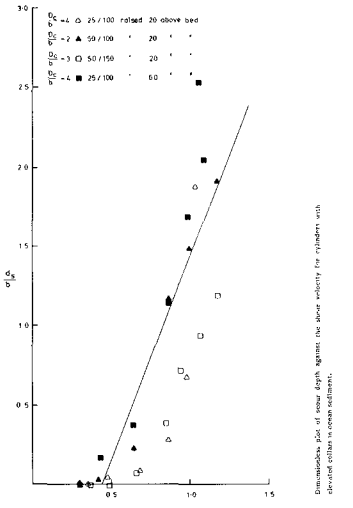

Dimensionless plot of scour depth against the above velocity for cylinders with elevated collars in ocean sediment.

FIGURE 10

5 DISCUSSION AND CONCLUSION

The work carried out in the present investigation has brought to light the importance of the parameter u_*/u_{*_c} for the determination of the depth of scour. It appears that the other parameter, the internal sediment Froude number, plays only a minor role. In order to test this hypothesis further, all available data from the literature for circular cylinders in model tests were reduced onto the same graph. Figure 11 is the resulting variation, with the data plotted being obtained directly from the publications of Breusers (1977), Chabert and Engeldinger (1956), Jain and Fischer (1980), Qadar (1981), Shen et al (1966) and of course the present results. The experimental data plotted in Figure 11 is listed in Table 2 and is from tests the details of which are included in Table 5. The soil types range from the present calcareous sediment with a $d_{50} \simeq 0.06$mm through sands varying in diameter from 0.2mm up to a maximum diameter of 3mm (test of Chabert and Engeldinger (1956)). This means that the range of u_{*_c} covered in Figure 11 is from about 12mmsec^{-1} to about 35mmsec^{-1}. Similarly the range of cylindrical pile diameters covered by the data is from 25mm to 200mm.

Only those data which represent ratios of flume depth to cylinder diameter of greater than 3 were included in the presentation. An exception to this case is some of the data from Shen et al (1966) which included ratios marginally smaller than three. However, these values were corrected for the smaller depth to diameter ratio by a formula suggested by Breusers et al (1977) who postulated the depth of scour to the depth to diameter ratio $d_s/b = 1.5 \tanh h/b$.

All the data show a very definite trend about the line of best fit derived from the sediment experiments (Figure 7). The scatter is not unusually severe for sediment transport or scour type experiments and it is believed that the most important correlation is captured in Figure 11. This means that the influence of different void ratios, soil structure and soil scour on the resistance is all provided for through the value of the critical shear velocity.

Unfortunately there is very little data available from larger laboratory experiments or from bridge pile monitoring of large depth to cylinder diameter ratios, and for values of u_*/u_{*_c} less than unity. The work by Qadar (1981) would indicate that the horseshoe vortex diameter is determined by the diameter of the cylinder and to a much smaller degree by the height of the bottom shear region. This would suggest that the present results should scale to prototype situations. However, the present results suggest a considerably larger vortex diameter than predicted by Qadar (1981).

TABLE 2

Test	Diameter	25mm	Test	Diameter	50mm	Test	Diameter	100mm
	u_*msec^{-1}	d_s mm		u_*msec^{-1}	d_s mm		u_*	d_s
SS8	0.0067	2	SS9	0.0071	0	SS10	0.0073	0
	0.0098	6		0.0103	5		0.0102	7
	0.0138	13		0.0145	24		0.0140	32
	0.0183	27		0.0187	47		0.0188	58
	0.0208	37		0.0219	64		0.0215	97
	0.0248	54		0.0240	78			
	0.0264	60		0.0264	96			
S13	0.0093	3	S9	0.0096	0	S19	0.0054	3
	0.0102	8		0.0103	10		0.0096	10
	0.0142	15		0.0140	30		0.0139	20
	0.0176	26		0.0184	50		0.0184	63
	0.0218	35		0.0221	60		0.0202	90
	0.0271	40		0.0247	75			
	0.0280	45		0.0277	95			
						S11	0.0097	15
							0.0187	95

Scour depths for ocean sediment bed for plain cylinder $u_{*c} = 0.023$msec^{-1}; water depth h = 0.307m; water temperature = 17.0°C (Mean); Sediment bed depth = 0.10m.

Scour depths for ocean sediment bed for cylinder with a collar at bed level:
u_{*_c} = 0.023msec^{-1}; water depth h = 0.307m; water temperature = 17.0°C (Mean);
Sediment bed depth = 0.10m.

TABLE 3

Test	Cylinder Diameter	25 mm	Test	Cylinder Diameter	50 mm	Test	Cylinder Diameter	100mm
	u_* ms^{-1}	d_s mm		u_* ms^{-1}	d_s mm		u_* ms^{-1}	d_s mm
S25 Collar D_c=75mm	0.0069	0	S21 Collar D_c=100mm	0.0091	0	S12 Collar D_c=200mm	0.0072	0
	0.0099	0		0.0105	2		0.0098	0
	0.0141	2		0.0141	20		0.0142	10
	0.0187	10		0.0184	30		0.0191	30
	0.0217	15		0.0209	35		0.0218	50
	0.0241	20		0.0237	45		0.0261	100
	0.0263	25		0.0265	55			
S24 Collar D_c=100mm	0.0078	0	SS12 Collar D_c=100mm	0.0080	0			
	0.0110	0		0.0107	3			
	0.0142	2		0.0148	9			
	0.0183	8		0.0188	28			
	0.0210	15		0.0212	35			
	0.0235	25		0.0241	41			
SS11 Collar D_c=100mm	0.0076	0	S10 Collar D_c=150mm	0.0093	2			
	0.0099	2		0.0135	10			
	0.0127	3		0.0180	30			
	0.0174	8		0.0222	30			
	0.0184	10		0.0247	30			
	0.0219	14		0.0278	30			
	0.0228	18						
			SS13 Collar D_c=150mm	0.0084	0			
				0.0109	0			
				0.0149	5			
				0.0180	14			
				0.0212	19			
				0.0234	24			
				0.0257	36			

TABLE 4

Test	Cylinder Diameter	25mm	Test	Cylinder Diameter	50mm
	u_*msec^{-1}	d_s mm		u_*msec^{-1}	d_s mm
SS14	0.0080	0	SS16	0.0069	0
Collar	0.0106	1	Collar	0.0092	2
D_c=100mm	0.0149	2	D_c=100mm	0.0141	12
Elevation	0.0193	7	Elevation	0.0180	58
20mm	0.0216	17	20mm	0.0218	75
	0.0231	45		0.0250	96
SS17	0.0069	0	SS15	0.0081	0
Collar	0.0097	4	Collar	0.0108	0
D_c=100mm	0.0141	9	D_c=150mm	0.0149	4
Elevation	0.0191	28	Elevation	0.0189	20
60mm	0.0218	42	20mm	0.0213	36
	0.0244	52		0.0237	47
	0.0264	63		0.0264	60

Scour depths for ocean sediment bed for cylinder with a raised collar:
u_{*_c} = 0.023msec^{-1}; water depth h = 0.307m; water temperature = 17.0°C (Mean);
Sediment bed depth = 0.10m.

TABLE 5

Author	Cylinder Diameter	Material	
	mm	Type	d_{50} mm
Breusers 1971	50 & 110	Sand	0.2
Chabert & Engelhinger 1956	50, 100 & 150	Sand Sand	0.52 1.5 3.0
Jain & Fischer 1980	516	Sand	0.29 0.50 0.63
Qadar 1981	25, 50 & 75	Sand	0.17 0.7 1.5
Shen, Schneider & Karaki 1966	150	Sand	0.24 0.46

Cylinder diameters and bed materials used by various other authors listed.

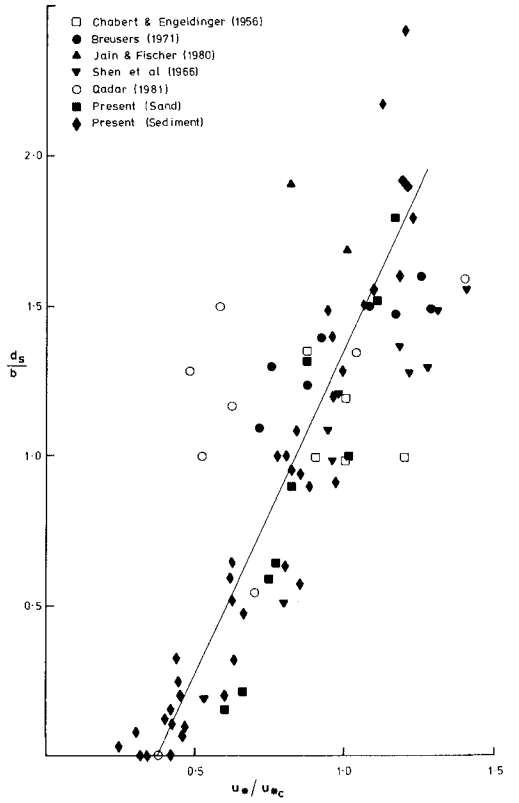

Dimensionless plot of scour depth against the shear velocity for cylinders without collars showing line of best fit from present results.

FIGURE 11.

The mechanisms for scour in the sediment and in the sand were discussed in section 4 where the very different nature of the two mechanisms was pointed out. In the case of sand, scour is achieved by the suspension of the material and subsequent slumping. By contrast, in the case of the sediment it appeared that the eddying in the horseshoe vortex caused local scour which deepened at first and then broadened to form a sheet like scour depression. The failure of the soil was much more hy lateral or horizontal scouring by the fluid as it swept past the near vertical sediment walls. There was very little evidence of the sediment slumping at any stage of the scour process. It is therefore quite remarkable that the sediment data and the sand data show the same correlation between d_s/b and u_*/u_{*_c}. This implies that, even though the mechanisms are different, it is the turbulent kinetic energy that is ultimately responsible for the scour. Similarly it is the single parameter u_{*_c} which determines the resistance of the soil to scour.

Installation of a protective collar hecame effective for collars at least twice the diameter of the cylinder. However, even for the large collars, scour holes formed and deepened to a depth comparahle to plain cylinders for u_*/u_{*_c} larger than unity, hut by the action of the wake rather than the horseshoe vortex. For collar diameters equal to twice the cylinder diameter the effect of the collar became negligible for d_s/b beyond a value of 1.5.

Acknowledgement

The authors would like to thank Woodside Offshore Petroleum Pty. Ltd. and the North-West Shelf Development Project Joint Venturers for funding and support of the research and Mr. R. Jewell for assisting in the design of the sample preparation technique.

BIBLIOGRAPHY

Breusers H.N.C., Nicollet G, & Shen H.W. 1977 — "Local Scour Around Cylindrical Piers". Journal of Hydraulic Research I.A.H.R. Vol 15 No. 3 1977

Breusers H.N.C. 1971 — "Local Scour Near Offshore Structures". Proc Symp on Offshore Hydrodynamics, Wageringen 1971 (also Delft Hydraulics Laboratory Publication No. 105).

Caldwell D.R. & Chris J.M. 1979 — "The Viscous Sublayer at the Seafloor" Science, 205, pp1131 to 1132.

Durand Claye, A.A. 1873 — Experiences sur les affouillements; Ann des Ponts et Chaussees, ler semestre, p467.

Carstens T & H.R. Sharma 1975 — "Local Scour Around Large Obstructions" Proc 16th I.A.H.R. Congress Sao Paulo, 2, pp251-262.

Chabert J & Engeldinger P 1956 — "Etude des affouillements autour des piles de ponts; Lab Nat D'Hydr Chatou Octobre.

Fugro 1981 — Report Nv: K-1052/XVIII

Jain S.C. & Fischer E.E. 1980 — "Scour Around Bridge Piers at High Flow Velocities" Proc A.S.C.E. HY11 November 1980, pp1827/1842.

Jain S.C. & Fischer E.E. 1979 — "Scour Around Bridge Piers at High Froude Number" Report No. FH-WA-RD-79-104. Federal Highway Administration Washington D.C. April 1979.

Jones H.A. 1973 — "Marine Geology of the Northwest Australian Continental Shelf" Bureau of Mineral Resources Bulletin 136.

Jewell R.J., Fahey, M. Wroth C.P. 1980 — "Laboratory Studies of the Pressure Meter Test in Sand". Geotechnique Vol XXX No. 5. December 1980.

Melville B.W. 1975 — "Local Scour at Bridge Sites" Rep No. 117 School of Engineering, University of Auckland, Auckland, N.Z.

Qadar A. 1981 — "The Vortex Scour Mechanism at Bridge Piers". Proc Inst'n Civil Engineers, Part 2, 1981, 71, September pp739-757.

Shen H.W., Schneider V.R. & Karaki S. 1966 — Mechanics of Local Scour; Supplement Methods of Reducing Scour, Colorado State Univeristy CER66 H.W.S. 36.

Tanaka S. & Yano M 1967 — "Local Scour Around a Circular Cylinder" Proc 12th I.A.H.R. Congress, Ft Collins 3 pp 193/201.

Vanoni V.A. ed 1975 — "Sedimentation Engineering" Manuals & Reports on Engineering Practice No. 54 A.S.C.E. 1975.

Zdenek T. 1967 — "An Interesting Hydraulic Effect Occuring at Local Scour. Proceedings I.A.H.R. Congres Vol. 3 Colorado September 1967.